Journal of Inflammation Research

Dovepress
Taylor & Francis Group

Open Access Full Text Article

ORIGINAL RESEARCH

Mechanism of Mongolian Medicine Batri-7 on *Salmonella* Enteritis

Dezhi Yang[1,*], Shana Chen[1,*], Haiyan Borijihan[1], Aoqier Aoqier[1], Sarula Sarula[1], Siqin Siqin[1], Manda Manda[1], Temuqile Temuqile[1], Huricha Baigude[1,2]

[1]National and Local Joint Engineering Research Center of Modern Mongolian Medicine Research and Testing, International Mongolian Hospital of Inner Mongolia, Hohhot, 010065, People's Republic of China; [2]School of Chemistry & Chemical Engineering, Inner Mongolia University, Hohhot, Inner Mongolia, 010020, People's Republic of China

*These authors contributed equally to this work

Correspondence: Temuqile Temuqile, International Mongolian Hospital of Inner Mongolia, Hohhot, Inner Mongolia, 010065, People's Republic of China, Tel +86 139-4711-9993, Email tmqyx01@163.com; Huricha Baigude, Institute of Mongolian Medicinal Chemistry, School of Chemistry & Chemical Engineering, Inner Mongolia University, Hohhot, 010020, People's Republic of China, Email hbaigude@imu.edu.cn

Purpose: Traditional Mongolian Medicine Batri-7 (BT-7) is the key Mongolian Medicine (MM) for bacterial enteritis. BT-7 is a well-known clinical MM due to its antibacterial properties. BT-7 contains plant-derived bioactive compounds, but its molecular mechanism of action remains unclear. This study explores BT-7's antibacterial compounds and therapeutic mechanism in a *Salmonella* enteritis mouse model.

Methods: The active components of BT-7 were detected by liquid chromatography-tandem mass spectrometry assay and identified by UPLC/Q-TOF-MS. An enteritis mouse model induced by *Salmonella typhimurium* was used in this study. Pathological analysis of small intestine was conducted with hematoxylin and eosin staining. The macrophage recruitment in model mice's intestines was detected by flow cytometry. Simultaneously, the Minimum Inhibitory Concentration of BT-7 was evaluated against bacterial by microbroth dilution method, BT-7 regulation of *Salmonella typhimurium* gene was performed by RNA-Seq methods and verified by qRT-PCR.

Results: In the LC-MS/MS assay, negative and positive-ion modes are identified for 511 and 699 compounds from BT-7, respectively. Of them, we found multiple antibacterial and anti inflammation compounds including chrysin, oroxylin A and luteolin. In vivo, we observed that treatment of mouse *Salmonella* enteritis with BT-7 decreases inflammation score and macrophages on intestinal tenue. In vitro, BT-7 presented the highest antibacterial activities against tested strains with MIC was 2–4 mg/mL. Meanwhile, BT-7 significantly down regulated *Salmonella* infection genes.

Conclusion: Twenty key anti-bacterial components were identified in the BT-7. In vivo experiment shows that orally administered BT-7 effectively reduce the inflammation of intestine in model of *Salmonella*-induced mouse enteritis by down regulating the infection-related virulence genes of *Salmonella*. Through this study, we discovered the mechanism of BT-7's dual action on the host and pathogenic bacteria. This gives inspiration for anti-infective disease research in traditional medicine and also proves that traditional medicines still have good prospects for treating infectious diseases.

Keywords: Mongolian medicine, Batri-7, antibacterial, *Salmonella* enteritis, virulence gene

Introduction

Salmonella is a gram-negative bacterium belonging to the Enterobacteriaceae family, and it is typically seen as a cause of gastroenteritis. There are around 2500 different species of bacteria in the *Salmonella* family. *Salmonella Typhimurium* and *Salmonella Enteritidis* are the main serotypes, causing about fifty percent of all human infections. *S. typhimurium* is commonly found in food of animal origin. *Salmonella enterica* often causes intestinal diseases, manifested as acute fever, abdominal pain, diarrhea, nausea, vomiting and other symptoms. According to the World Health Organization (WHO), there are approximately 93.8 million cases of gastroenteritis worldwide each year that can be linked to *Salmonella* infections. Additionally, *Salmonella* infections are responsible for causing 155,000 deaths.[1]

Received: 4 October 2024
Accepted: 27 January 2025
Published: 3 February 2025

Traditional medicine is commonly used for treating bacterial infections, and numerous drugs have demonstrated antibacterial abilities against Drug-Resistant Bacteria.[2,3] Traditional Mongolian Medicine "Batri-7" (denoted by BT-7) is widely used for the treatment of bacterial infection in clinics practicing traditional medicine, where it is known as 'antibiotics' of Mongolian Medicine. It was a classic prescription included in *The Drug Standards of the Ministry of Health of the People's Republic of China*. BT-7 formulation is composed of seven natural products including *Aconitum kusnezoffii* (*Aconitum* L., *A. kusnezoffii* leaf; Mongolian name: Bongaa in Nabqi), *Potentilla discolor* Bge. (*Potentilla* L., *Potentilla discolor* Bge. whole plant, Mongolian name: Alag Toolai in Tangnaii), *Commiphora muku* (*Commiphora, Commiphora muku* resin, Mongolian name: Gugule*), Terminalia chebula* Retz. (*Terminalia* L., *Terminalia chebula* Retz. dry fruit, Mongolian name: Arura), Artificial Moschus (Mongolian name: Jagaar), and cinnabar (*cinnabaris*, Mongolian name: Xinghu)[4,5] (Table 1 and Figure 1).

In Mongolian Medicine, an invisible pathogen passes through the mouth, sweat glands, nasal cavity to infect human body and cause the "Nian" disease.[6] In the clinic, BT-7 has significant therapeutic effects on "Nian" disease, especially on gastrointestinal "Nian", especially the treatment of bacterial enteritis has been proven in clinical practice. Although many studies have shown that traditional medicines have antibacterial effects,[7,8] the under lying mechanism of Mongolian medicine ingredients and their efficiency on pathogenic bacteria are not clear yet.

In this study, the rule of Mongolian medicine BT-7 treating on *Salmonella* enteritis was analyzed by enteritis mouse model induced by *Salmonella typhimurium*, and potential main components to treat *Salmonella* enteritis were screened through LC-MS/MS and network pharmacology, and the mechanism of BT-7 against *Salmonella typhimurium* was further revealed through in-vitro anti-bacterial experiments and RNA-seq.

Materials and Methods

Reagents and Instruments

Batri-7 (M20201011) was provided by the Formulation Center, International Mongolian Hospital of Inner Mongolia, Hohhot, China. Methanol (Thermo), Forate (Thermo), Ammonium acetate (Thermo). Waters Acquity UPLC/qTOF includes quaternary solvent manager, online degasser, sample manager, column manager, Acquity PDA detector, ESI source, Lockspray source, Xevo G2-XS QTof four-pole flight time tandem mass spectrometer and Masslynx V4.1 Workstation. Acetonitrile is purchased from Fisher Scientific, USA. Additional chemicals was obtained from Guoyao Chemical Reagent Co. Ltd. Q ExactiveTM HF (Thermo Fisher), Vanquish UHPLC (Thermo Fisher), Hypersil Gold column (Thermo Fisher), Centrifuge ST16R (Scilogex).

Preparation of Semi-Bionic Extraction of Batri-7 (BT-7-SBE)

Preparation of BT-7-SBE were performed using methods modified from previous research.[9,10] Briefly, Batri-7 (90 g) were powdered and extracted two times with stirring and heating (37 ± 0.5°C), the extraction procedure of the first was 7 times the amount of simulated gastric fluid (Sodium taurocholate 80 μM, Lecithin 20 μM, Pepsin 0.1 mg/mL, NaCl 34.2

Table 1 The Whole Botanical Name and Voucher Number of the Plant Ingredient in Batri-7[a)]

Full Botanical Name	Part Used	Voucher Number	Family	Content (g; %)
Aconitum kusnezoffii Reichb.	Leaf	T000200065	Ranunculaceae	25; 27.3
Terminalia chebula Retz.	Fruit	T001800344	Combretaceae	25; 27.3
Potentilla discolor Bge.	Whole plant	T000200238	Rosaceae	10; 10.9
Commiphora mukul (Hook.ex Stocks) Engl.	Resin	T150202310	Burscraccae	10; 10.9
Rubia cordifolia L.	Stems, leaves	T001100612	Rubiaceae Juss.	10; 10.9

Notes: [a)]Batri-7 contains 12.7% of non-plant substances, including Musk gland (T001600693, 1.5 g, 0.02%) and Cinnabar (T001400907, 5 g, 0.05%). The traditional process for preparing the BT-7 pill involves grinding all the ingredients, which include both plant and non-plant ingredients, into a fine powder. The powder is then passed through a mesh strainer to remove any bigger fragments. In order to generate a dense paste, water was gradually included into the mixture. The resulting mixture was then vigorously kneaded using a mortar in a bowl and tightly compressed to ensure thorough blending. The mixture was shaped into a slender cylinder. The roll was subsequently sliced to a length of two-three millimeter and small pills, similar in size to a soy bean, were formed and then dried in the oven at a temperature of within 35°C for a duration of two hours. Voucher number from Traditional Chinese medicine decoction pieces https://code.nhsa.gov.cn/yp/toRkList.html.

Figure 1 Plant originated components of BT-7.

mM and pH = 1.6) and extraction times were 2 h. The second was 4 times the amount of simulated intestinal buffer (Sodium taurocholate 3 mM, Lecithin 0.75 mM, NaH_2PO_4 3.438 g, NaCl 6.186 g and pH = 7.0) and extraction times were 2 h. The solution was centrifuge, filtered, mixed and concentrated, and 21.1 g of a brown powder was obtained and dissolve to DMSO at final concentration at 70 mg/mL.

LC-MS/MS Analysis

The Liquid chromatography tandem mass spectrometry (LC-MS/MS) studies were carried out at Novogene Co., Ltd. (Beijing) using a Vanquish UHPLC system (Thermo Fisher) connected to an Orbitrap Q ExactiveTMHF-X mass spectrometer (Thermo Fisher). The samples were loaded onto a Hypersil Gold column using a 17-minute linear gradient at a flow rate of 0.2 mL/min. The eluents used in the positive polarity mode were eluent A, which consisted of 0.1% formic acid in water, and eluent B, which consisted of methanol. The eluents used for the negative polarity mode were eluent A, consisting of a solution containing 5 mM ammonium acetate at pH 9.0, and eluent B, consisting of methanol. The solvent gradient was set as follows: 2% B, 1.5 min; 2–85% B, 3 min; 85–100% B, 10 min; 100–2% B, 10.1 min; 2% B, 12 min. The Q ExactiveTM HF-X mass spectrometer was used in positive/negative polarity mode with a spray voltage of 3.5 kV. The capillary temperature was set to 320°C, the sheath gas flow rate was 35 pressure, and the auxiliary gas flow rate was 10 L/min. The S-lens RF level was set to 60, and the auxiliary gas heater temperature was 350°C.

https://doi.org/10.2147/JIR.S491957

Network Analysis

The chemical compositions of BT-7 were analyzed using LC-MS/MS. The selection requirements for these compositions were a Percent Human Oral Absorption rate of at least 30% and a drug likeness (DL) value of at least 0.185. The chemical targets of BT-7 have been downloaded from the TCMSP database, which is a database and analysis platform for traditional Chinese medicine systems pharmacology (https://old.tcmsp-e.com/tcmsp.php). The disease targets of enteritis with inflammation were obtained from the Gene Cards Database (https://www.genecards.org), National Center of Biotechnology Information database (NCBI) (https://www.ncbi.nlm.nih.gov/), and Online Mendelian Inheritance in Man database (OMIM) (https://omim.org/). The UniProtKB query tool within the UniProt database was applied to standardize the names of the expected target genes (http://www.uniprot.org/).At last, a Venn analysis was carried out on the BT-7 and enteritis with inflammatory target genes in order to determine those common target genes. These target genes were used for the Gene Ontology (GO) (http://www.geneontology.org/) and Kyoto Encyclopedia of Genes and Genomes (KEGG) pathway (www.kegg.jp/kegg/pathway.html) analysis. Finally, using Cytoscape 3.9.0 a protein–protein interaction (PPI) network was constructed for the main pathway-related genes and metabolic components.

Molecular Docking

This study identified a significant target within the "Component Target-Pathway network" for targeted proteins, together with the six highest-degree active components from Cytoscape 3.9.0, to conduct molecular docking and validate their interaction activity. The protein crystal structure used for docking was sourced from the Protein Data Bank (PDB), while the 3D structures of the small molecules were retrieved from the PubChem database. The energy is optimized utilizing the MMFF94 force field. The molecular docking analysis was conducted using AutoDock Vina version 1.2.3 software. Before the commencement of docking, all receptor proteins were processed using PyMol 2.5.5, which entailed the elimination of water molecules, salt ions, and small molecules. Thereafter, the docking box is defined, and PyMol determines the precise central location of the box to ensure that each pocket within it serves as a possible binding site. Furthermore, all modified small molecules and receptor proteins were converted into the necessary PDBQT format for docking with autoDock Vina 1.2.3 utilizing ADFRsuite 1.0. In the docking phase, an extensive global search was performed with a thoroughness level set at 32, while all other parameters remained at their standard settings. The docking confirmation with the highest score from the output was utilized as a combination of confirmation, and the docking result from PyMol 2.5.5 was employed for visual evaluation.

Analysis of UPLC-QTof-MS

The following chromatographic conditions were used for detection: The Waters ACQUIY UPLC® BEH Shield RP18 column was linked to a Vanguard HSS T3 guard column. Column temperature was 40°C; the mobile phase was as following: A: water (with 0.1% formic acid), B: acetonitrile (with 0.1% formic acid); the mobile phase gradient elution was: 50% → 90% B, 10 → 15 min: 100% B, 15 → 20 min: 50% B; the flow rate was 0.4 mL/min; the injection volume was: 2 μL. The experimental parameters for the mass spectrometry were as follows: The analysis method performed was Electrospray Ionization in the positive ion mode. Mass detection range was 100–1200 Da; capillary voltage was 3 kV; sample cone was 40 V; extraction cone was 4 V; source temperature was 100°C; desolvation temperature was 400°C; desolvation gas was 800 L/h, lockmass was 556.2771. The threshold for accuracy inaccuracy was set at 5 milliDaltons. The MassLynx 4.1 software controls the process of data collecting. The chemical composition of BT-7, which has antibacterial activity, was analyzed using LC-MS/MS detection. The chemical constituents were identified and their structures were determined using the "Chemdraw" software is utilized for generating of a molecular formula and a database as well as theoretical relative molecular masses.

Determination of Minimum Bactericidal Concentration of BT-7

For the MIC test, A two-fold serial dilution method was applied to obtain different concentrations of BT-7 's antibacterial activity. At the 96-well plates, 100 μL of 10^4 cells of Salmonella typhimurium (14028s), Listeria monocytogenes (ATCC19111), and Staphylococcus aureus (ATCC 25923) were added into the culture with

different concentrations of BT-7. The plates were incubated at 37°C for 24 hours. Then, dilution cell to 10^2 cells from the mixture in each well was plated on solidified LB agar and incubated at 37°C for 24 hours to obtain the MIC. No growth on LB-agar was observed in the MIC. The MIC was defined as the lowest concentration of BT-7 with bactericidal activity against the indicator strain.[11] All experiments were conducted in triplicate.

Animal Experiment

Female mice, ages five weeks, weighing between 30 and 40 g, were purchased from Beijing Si Pei Fu Laboratory Animal Technology Co. Ltd. These mice were free from any specific pathogens. The mouse was acclimated for a period of 7 days prior to the beginning of any examinations. They were housed in a controlled environment (4 animals per cages, 55 ± 5% relative humidity, 22°C, 12 h:12 h light/dark cycle) and provided with free access to food and water. In vivo infection with Salmonella was carried out as described.[12] Briefly, mice were treated with streptomycin at 300 mg/liter in drinking water for 2 days. Control mice were administered antibiotic-free drinking water. After 2 days, the antibiotics were withdrawn, and mice were infected with 3×10^8 Salmonella serovar Typhimurium (ATCC 14028) CFU/mouse by oral gavage. Uninfected control mice were given the same volume of PBS. For treatment experiments, mice were randomly divided into five groups and were continuously oral administration medicines, positive control (Levofloxacin) and BT-7 by oral administration (once a day) for 5 days. The doses for each group were as following: untreated group (NT, n = 5, saline), Enteritis (Model, n = 5, saline), Enteritis+ Levofloxacin (EL, n = 5, Levofloxacin, 8 μg/100 g body weight), Enteritis+ BT-7 low (BT-7 low, n = 5, BT-7 35 mg/100 g body weight), and BT-7 high (BT-7 high, n = 5, BT-7140 mg/100 g body weight). Drug doses were determined according to the dose of BT-7 in clinic: the dose of BT-7 low is 5 times of dose for human; the dose of BT-7 high is 4 times of BT-7 low. Mice were sacrificed by cervical dislocation and all studies were approved by the Ethics Committee of Inner Mongolia International Mongolian Hospital (Issue No. 2022–001) and all experiments, which were performed in accordance with the National Institutes' Guidelines for the Care and Use of Laboratory Animals.

H&E Staining

The Hematoxylin and Eosin (H&E) Staining procedure was performed using a methodology that has been previously described.[13] The intestinal tissues were preserved by immersing them in a solution of 10% neutral buffered formalin for a whole night, followed by transferring them to a solution of 75% ethanol. The tissues were stained with H&E using the Modified Hematoxylin-Eosin HE Stain Kit, following usual procedures (Solarbio). Pathological scores were assigned as similar method that has been published previously.[14] A scoring system was employed as follows: The numerical scale used to classify the severity of the condition is as follows: 0 indicates a normal state; 1 indicates villi blunting and mucosal inflammation; 2 indicates villi blunting, extensive mucosal inflammation, and submucosal inflammation; 3 indicates significant submucosal inflammation; and 4 indicates transmural inflammation.

Flow Cytometry Analysis

For macrophages counting, the equal weight intestinal tissues into small pieces, which were serially incubated in 1 × HBSS containing 5% FBS and 2 mM EDTA, and digestion buffer (1 × HBSS supplemented with 5% FBS, collagenase VIII, and DNase I). The released cells filtered through a 40-mm cell strainer and stained with FITC-conjugated anti- mouse F4/80 (BioLegend Cat. No. 123108, 1:100), PE-conjugated anti-CD11b (BioLegend Cat. No. 101208, 1:100) for 30 min at 4°C in the dark and resuspended in FACS buffer. Flow cytometric analysis was performed on a FACSCantoII (BD Biosciences, San Jose, CA, USA), and the data were analyzed with BD FACSDiva software.

RNA Sequencing (RNA-Seq) and Quantitative RT-PCR

Salmonella total RNA was isolated with a RNAprep Pure Cell/Bacteria Kit (Tiangen), according to the manufacturer's instructions. mRNA was purified from total RNA using probes to remove rRNA. First strand cDNA was synthesized using random hexamer primer and M-MuLV Reverse Transcriptase, then use RNaseH to degrade the

RNA, and in the DNA polymerase I system, use dUTP to replace the dNTP of dTTP as the raw material to synthesize the second strand of cDNA. Remaining overhangs were converted into blunt ends via exonuclease/polymerase activities. After adenylation of 3′ ends of DNA fragments, Adaptor with hairpin loop structure were ligated to prepare for hybridization. Then, USER Enzyme was used to degrade the second strand of cDNA containing U, in order to select cDNA fragments of preferentially 370–420 bp in length, the library fragments were purified with AMPure XP system (Beckman Coulter, Beverly, USA). Then PCR was performed with Phusion High-Fidelity DNA polymerase, Universal PCR primers and Index (X) Primer. At last, PCR products were purified (AMPure XP system) and library quality was assessed on the Agilent Bioanalyzer 2100. The clustering of the index-coded samples was performed on a cBot Cluster Generation System using TruSeq PE Cluster Kit v3-cBot-HS (Illumia) according to the manufacturer's instructions. After cluster generation, the library preparations were sequenced on an Illumina Novaseq platform and 150 bp paired-end reads were generated. Genes that exhibited a >1.5-fold change in expression, as determined by at least two pairwise comparisons showing the same trend, were chosen for further study in the test phase ($p < 0.01$). For RT-PCR, synthesized cDNA through a reverse transcription reaction using EasyScript® First-Strand cDNA Synthesis SuperMix (TransGen Biotech), which we then amplified with TransStart® Green qPCR UDG (TransGen Biotech) on an ABI Prism 7500 System (ABI, Carlsbad, USA). All oligonucleotides were purchased from Syn-Biotech.

Statistical Analysis

Data processing was undertaken with GraphPad Prism 6 software (La Jolla, USA). Continuous variables are described by mean ± standard deviation (mean ± SD). For independent samples, a two-tailed Student's *t*-test was used for two-group comparisons, while multiple groups were compared with one-way analysis of variance (ANOVA) followed by Tukey's post-hoc test for pairwise comparisons. The results were considered statistically significant when the *p*-value was less than 0.05.

Results

Chemical Composition of BT-7

To identify the key chemical composition of BT-7-SBE, we use the LC-MS/MS assay. Figure 2A and B illustrate that we identified 511 compounds in the negative (NEG) electrospray ionization modes of UHPLC-QE-MS, and 699 in the positive (POS) electrospray ionization modes. A total of 1210 chemical components were identified, with 78 types of chemicals classified as flavonoids, terpenoids, phenylpropanoids, phenols, and alkaloids being the primary chemical

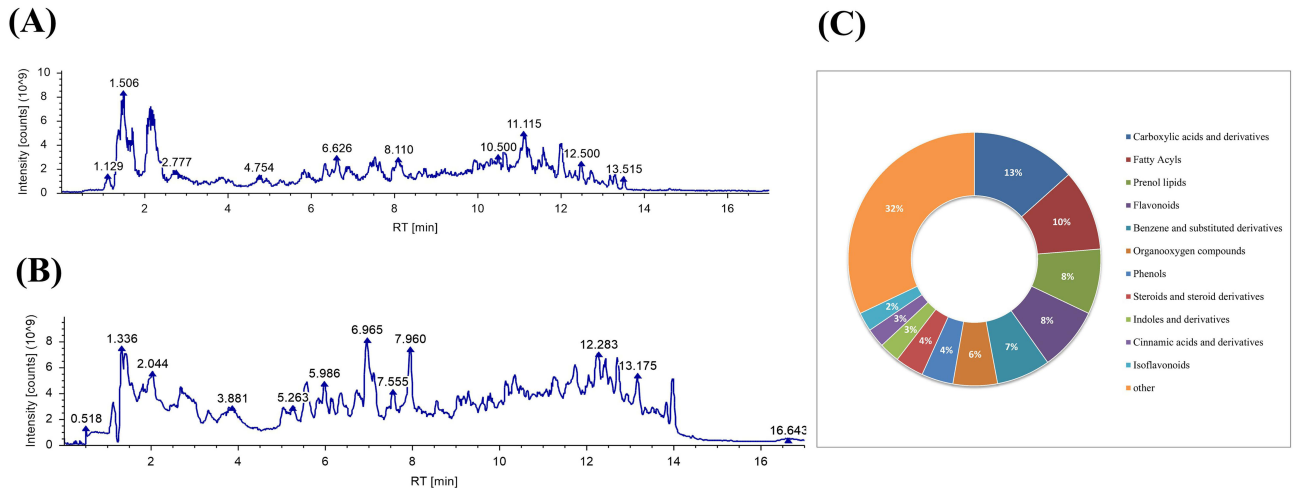

Figure 2 Analysis of active components of BT-7-SBE. (**A**) UHPLC-QE-MS BPI chromatogram of BT-7 extracted under the negative (NEG) electrospray ionization mode. (**B**) UHPLC-QE-MS BPI chromatogram of BT-7 extracted under the positive (POS) electrospray ionization mode. (**C**) Classification of active components of BT-7 detected by UHPLC-QE-MS analysis.

constituents of BT-7-SBE (Figure 2C). These compounds are common in medicinal plants, and many of them have been confirmed with anti-inflammatory and anti-bacterial activities.

Searching for the Anti-Inflammatory Target of BT-7 with Network Pharmacology

The network analysis "Compound-Target-Disease" is appropriate to explore the complicated TMM therapeutic effects of multiple compounds and targets. Therefore, we performed a network analysis of the BT-7 metabolites that had been detected by the LC-MS/MS assay to explore the pharmacological actions of BT-7. In the TCMSP database, we obtained 146 BT-7 components that were screened according to the Percent Human Oral Absorption (≥30%) and DL values (≥0.18). Meanwhile, there were 883 target genes related to the BT-7 components. There were 420 enteritis-inflammation target genes obtained from the Gene Cards, NCBI, and OMIM Databases. Using the Venn analysis, we identified 82 common target genes among the BT-7 and enteritis-inflammation-related target genes (Figure 3A). In order to obtain more insight into the complex connections underlying components, diseases, and their respective targets, we created a network that covers the included components, therapeutic diseases, and its effect on the targets. We imported it into Cytoscape 3.8.0 to create a graphical illustration of the network (Figure 3B). GO and KEGG enrichment analyses were conducted on these 82 target genes. The 82 of BT-7's target genes for enteritis-inflammation treatment were introduced into String 11.5 to construct a PPI network, and the top 20 key genes were screened according to their degree value (ALB, IL6, AKT1, TNF, VEGFA, TP53, MAPK3, CXCL8, MAPK1, PTGS2, EGFR, CASP3, SRC, MMP9, JUN, MAPK8, AR, RELA, APP and HIF1A). GO analysis indicated that these components significantly regulated the oxidative stress, chemical stress, response to molecules of bacterial origin, cell signaling transduction, and cell structure like membrane and synapse (Figure 3C). In the KEGG enrichment analysis, most of the target genes were significantly enriched in the pathogen infection, inflammatory signaling pathway, such as lipid and atherosclerosis, TNF signaling pathway, Toll-like receptor signaling pathway, and lL-17 signaling pathway (Figure 3D).

Molecular Docking of Key Active Components of BT-7 with Inflammation Target

Applying docking simulation technology offers a convenient and efficient method to investigate the interaction between small compounds and target proteins. In this study, we apply the Vina 1.2.3 software to discover the binding affinity and binding pattern of the active components (chrysin, ladanein, luteolin, moslosooflavone, oroxylin A and tectochrysin) between protein TNF-α. The binding mode of chrysin to TNF-α protein is shown in Figure 4. Chrysin forms a pi–pi interaction with TYR-135 on TNF-α protein and forms hydrophobic interaction with TILE-231, LEU-233, TYR-135 and LEU-133 on the TNF-α (Figure 4A). Ladanein and protein on ILE-231, LEU-233, TYR-135 and LEU-133 form a hydrophobic effect and hydrogen bond with LEU-233, in addition, form a pi–pi interaction with TYR-135 of TNF-α (Figure 4B). The attachment pattern and action details of luteolin to TNF-α protein have been shown in the figure below (Figure 4C), and ILE-231, LEU-233, TYR-135, LEU-133 of TNF-α form hydrophobic effects with luteolin and also form hydrogen bonding and pi–pi interaction with LEU-233 and TYR-135. The binding mode of moslosooflavone with TNF-α protein is shown in the figure below (Figure 4D), and the moslosooflavone forms a hydrophobic effect with TNF-α on ILE-231, LEU-233, TYR-135, LEU-133 and forms pi-pi interaction with TYR-135. Oroxylin A and TNF-α on ILE-231, LEU-233, TYR-135, LEU-133 form hydrophobic effects and form hydrogen bonding with TYR-195, and pi–pi interaction with TYR-135 (Figure 4E). Tectochrysin with TNF-α at ILE-231, LEU-233, TYR-135, LEU-133 form hydrophobic effect, and at TYR-227 form hydrogen bond, in addition, with TYR-135 to form pi–pi interaction (Figure 4F). TNF-α is a key target, and most molecules have strong binding energy with TNF-α on the ILE-231, LEU-233, TYR-135, LEU-133, and other amino acids are frequent amino acids that interact with these molecules, which means that these amino acids are key amino acids of TNF-α.

Analysis of Anti-Bacterial Components in BT-7

The BT-7 compound consists of several active components with broad inhibitory effects on both gram-positive and gram-negative bacteria. By applying the method of UPLC-qTOF mass analysis, we successfully detected a total of 20 compounds in the BT-7-SBE that have the potential to exert important antibacterial effects (Figure 5A–E). These compounds were previously reported to have antibacterial activity (Table 2).

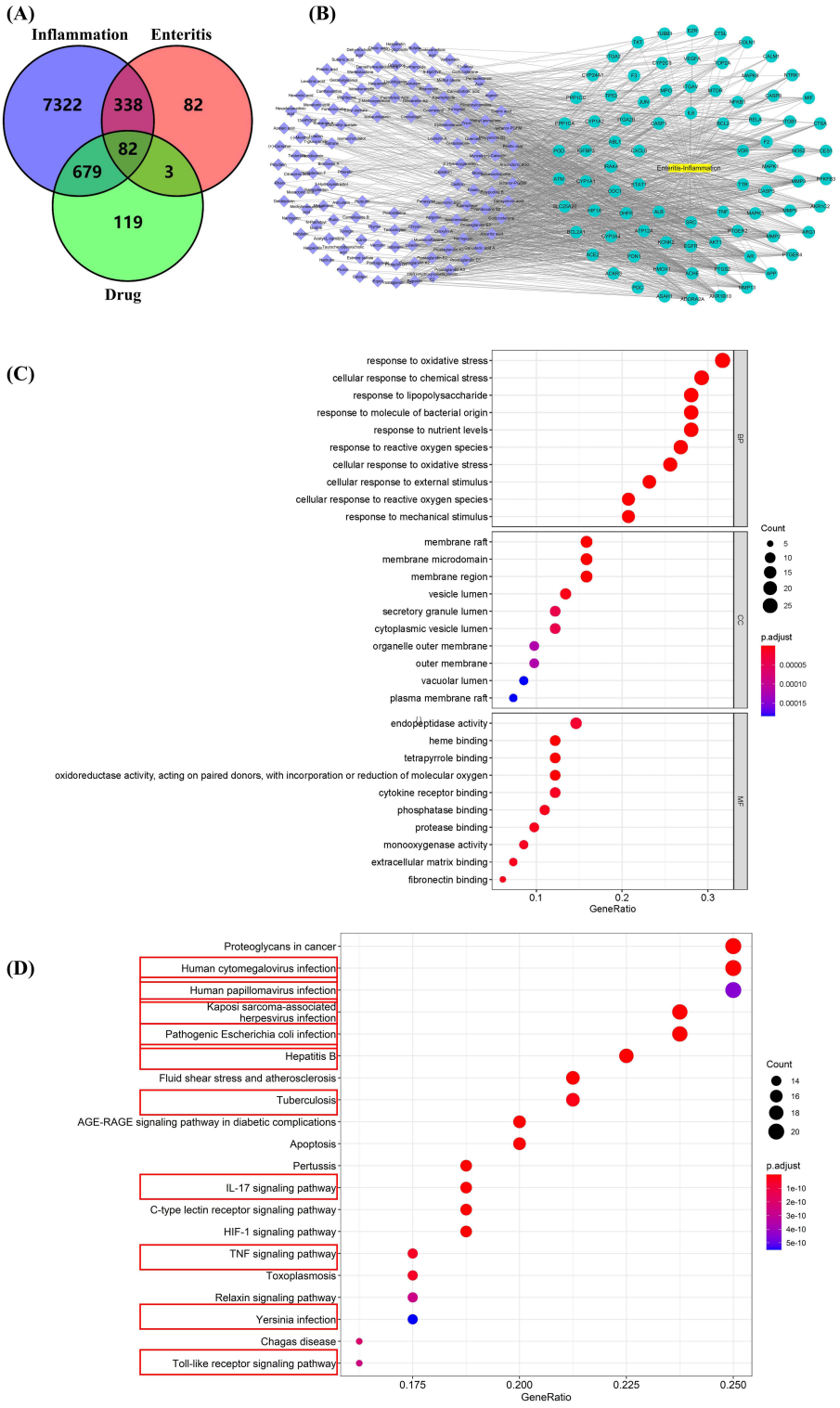

Figure 3 A comprehensive investigation of the network pharmacology of enteritis with inflammation with BT-7. (**A**) The Venn diagram illustrates the shared target genes between drugs and diseases. The size represents the quantity of target genes. The blue and red circle represents the target genes associated with enteritis and inflammation. The green circle represents the target genes of the 146 components of UHPLC-QE-MS in BT-7. The overlapping area represents the shared target genes. (**B**) Compound-active ingredient-disease-target gene. Node colors represent different groups: The light purple circle in the network represents the active components, green represents the target of the drug acting on the disease, and yellow represents the disease. The connecting line represents the network relationship between the compound and the target. (**C**) GO analysis (top 20), Biological process (BP), cellular component (CC), and molecular function (MF). (**D**) Performing KEGG analysis to identify the top 20 enriched pathways. The size of each node indicates the number of target genes that are enriched, while the color of the node ranges from blue to red, indicating the *p*-value from high to low. The length of the node corresponds to the number of target genes that are enriched, meanwhile the color of the node ranges from blue to red, indicating the p-value from high to low.

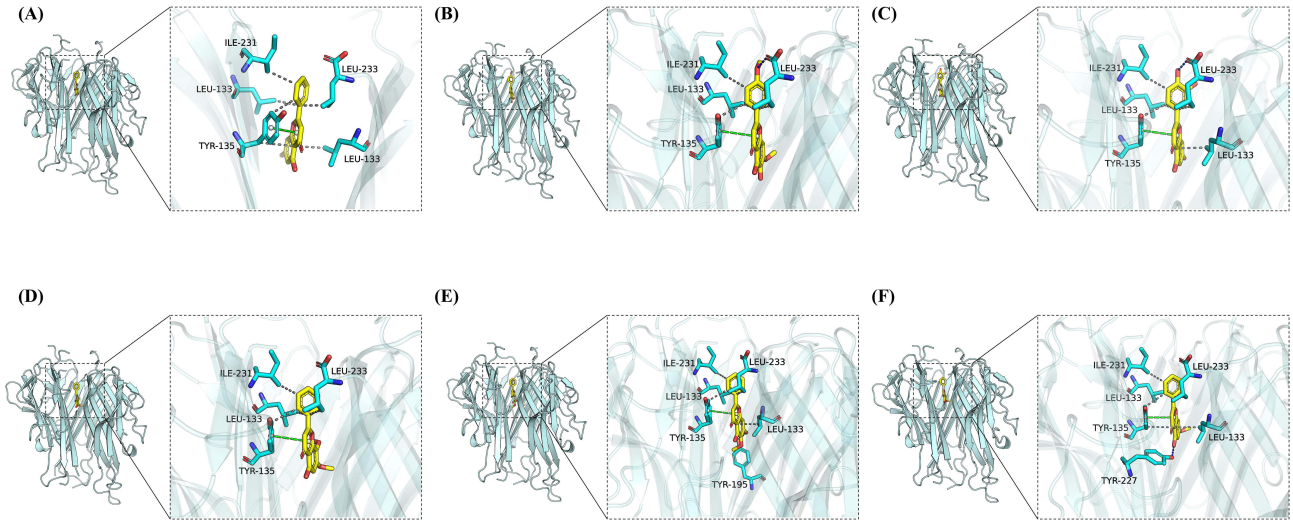

Figure 4 Molecular docking of BT-7's six key components with TNF-α. (**A**) Chrysin and TNF-α binding mode, (**B**) Ladanein and TNF-α binding mode, (**C**) Luteolin and TNF-α binding mode, (**D**) Moslosooflavone and TNF-α binding mode, (**E**) Oroxylin A and TNF-α binding mode, (**F**) Tectochrysin and TNF-α binding mode.
Note: The illustration on the left provides a comprehensive perspective, while the illustration on the right offers a limited viewpoint. The yellow stick symbolizes a component, the blue cartoon symbolizes proteins, the blue line symbolizes hydrogen bonding, the gray dashed line symbolizes hydrophobic interactions, and the green dashed line symbolizes pi–pi interactions.

Antibacterial Activity of BT-7

The primary antimicrobial screening was carried out using the medium dilution method. As showed in Figure 6A and B, BT7-SBE (0–3.5 mg/mL) inhibited the growth of *Salmonella* dose dependently, reaching a complete growth inhibition at a concentration of 3.5 mg/mL. Minimal inhibitory concentration (MIC) of BT7-SBE against the *Salmonella typhimurium, Listeria monocytogenes* and *Staphylococcus aureus* were summarized in Table 3.

BT7 Attenuated the Invasion of S. typhimurium in Mice

To investigate the in vivo antibacterial activity of BT-7, H&E-stained intestine were examined on the *Salmonella typhimurium*-induced intestinal infection model of mice (Figure 7A and B). H&E staining showed that the intestine of *Salmonella* infected mice treated with BT-7 significantly reduced edema and inflammatory infiltration, and at the higher dose completely protected the epithelial architecture (Figure 7C and D, $^{**}p<0.01$, $^{***}p<0.001$).

BT-7 Inhibit Arginine Synthesis Pathway and Infection Genes in Salmonella

At a concentration of 1/2 MIC in BT-7, around 20% of bacteria survive. To understand the mechanisms by which interaction with BT-7 we conduct RNA-Seq experiments. Here, 1/2 MIC of BT-7 was used to treat *Salmonella* cells, and non-treated bacteria were used as control. Among all the identified differentially expressed genes (DEGs), 1547 genes were significantly downregulated, while 1522 genes had the significantly upregulated (Figure 8A, $p < 0.05$). The majority of DEGs were present in all replicates (Figure 8B). To assess the biological implications of DEGs we identified, we conducted KEGG pathway enrichment analyses. The top 20 up- and down-regulated pathways are shown in Figure 8C and D. Top 3 up-regulated DEGs were enriched in pathways controlling ATP-binding cassette (ABC) transporters, oxidative phosphorylation and o-Antigen nucleotide sugar biosynthesis, while downregulated genes were enriched in pathways controlling arginine biosynthesis, *Salmonella* infection and sulfur metabolism. The interaction between the *Salmonella* infection pathway and pharmacological analysis confirmed the role of BT-7 (Figure 8D). Therefore, some infection-related genes were randomly selected from the down-regulated genes in the *Salmonella* infection pathway for confirmation by RT-PCR (Figure 9).

https://doi.org/10.2147/JIR.S491957

Discussion

The World Health Organization (WHO) reports that over 2 billion individuals worldwide face diarrhea each year.[37] The abuse of antibiotics in recent years has resulted in a growing worldwide challenge of bacterial resistance. It is urgently needed to find efficient, low toxicity, and anti-drug resistant bacteria drugs.[38] More and more research has shown that traditional medicines have direct antibacterial effects or promote the antibacterial activity of antibiotics, with relatively small adverse reactions and less susceptibility to drug resistance.[3] Natural medicine resources are characterized by a wide

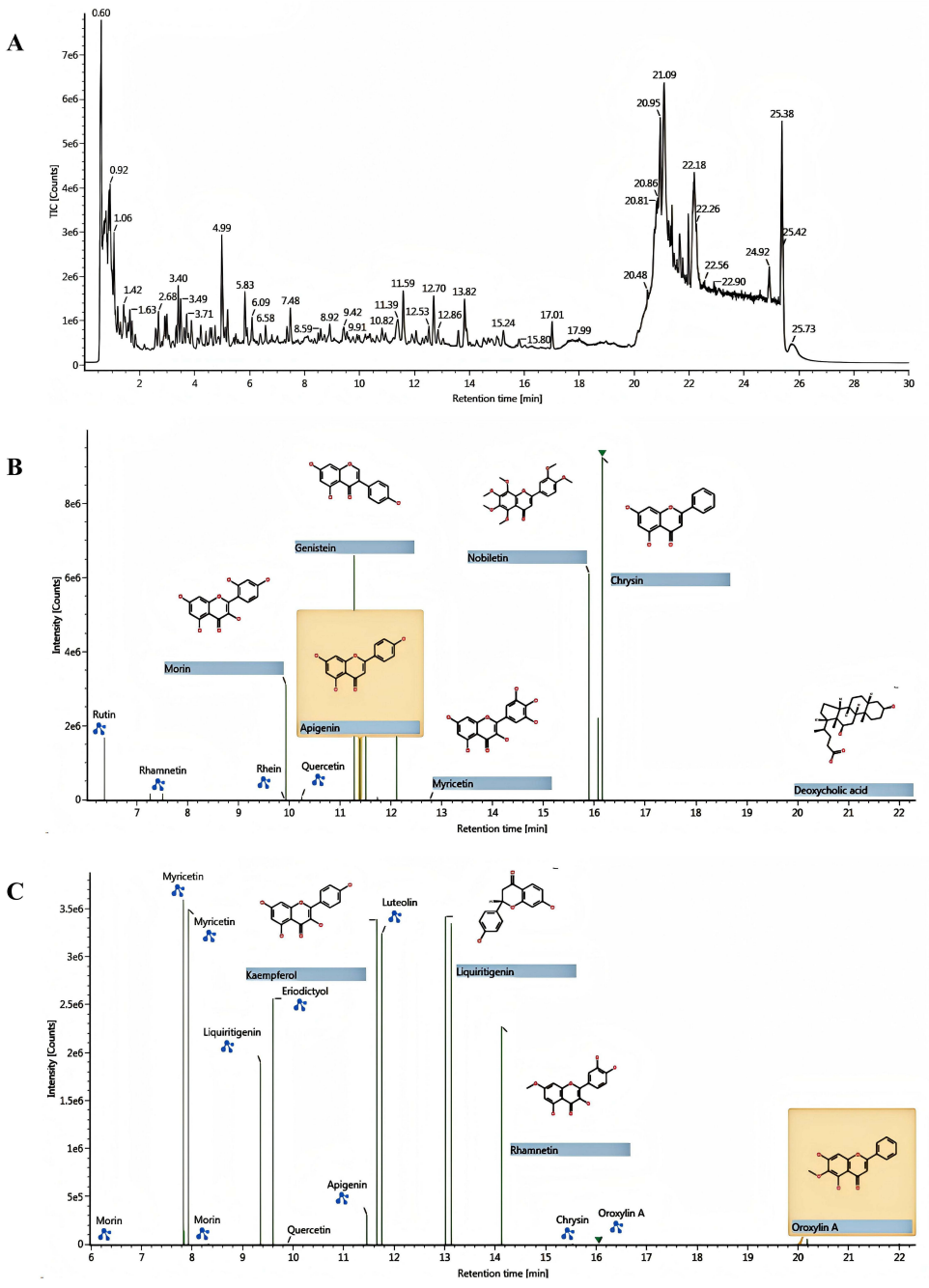

Figure 5 Continued.

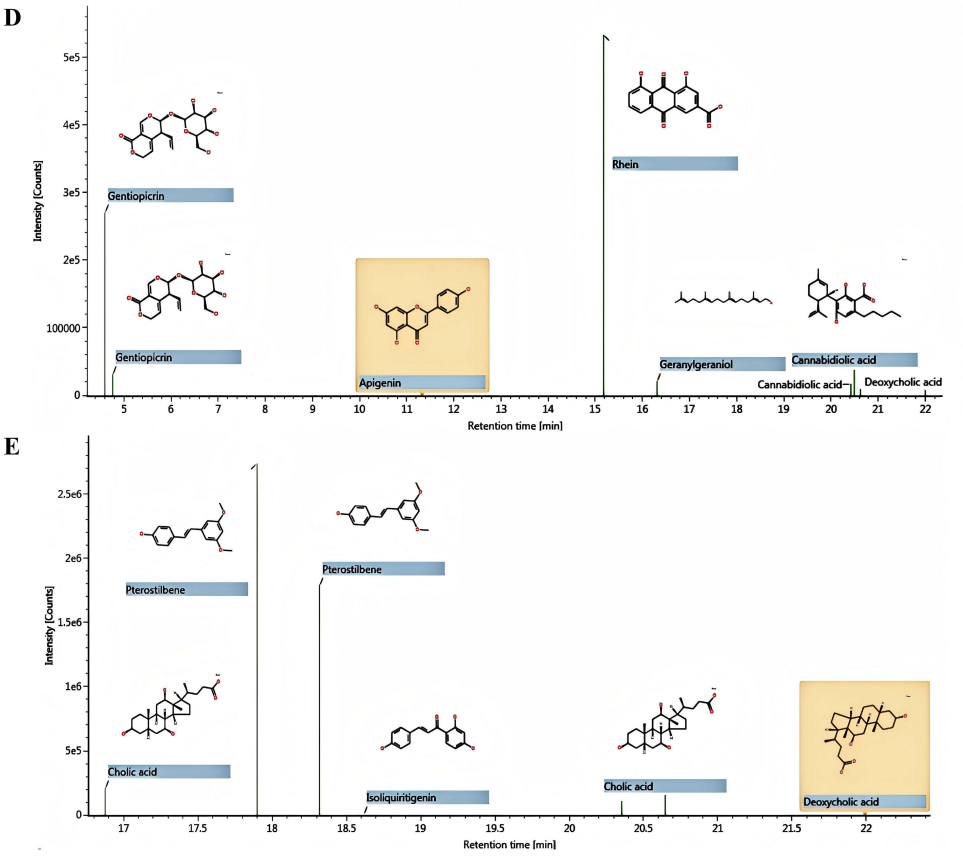

Figure 5 Analysis of active components of BT-7. (**A**) UHPLC-QE-MS BPI chromatogram of BT-7's main anti-bacterial components. Plots of identified anti-bacterial components extracted from BT-7SBE using UHPLC-QE-MS and UNIFI data processing. (**B**) MS/MS spectrum of morin, genistein, quercetin, myricetin, nobiletin, chrysin and deoxycholic acid. (**C**) MS/MS spectrum of kaempferol, liquiritigenin, rhamnetin and oroxylin A. (**D**) MS/MS spectrum of apigenin, rhein and geranylgeraniol. (**E**) MS/MS spectrum of cholic acid, pterostilbene and isoliquiritigenin.

range of drug sources. Therefore, searching for new antibacterial drugs from traditional medicine has become a new opportunity.[39] This study explores antibacterial mechanism research in Traditional Mongolian Medicine formulas BT-7.

We observed the toxicity of BT-7 in pre-experiments by gavage with a dose of BT-7 equivalent to 5 times the highest dose used in this study, which did not cause toxicity or death in mice, and other studies have also reported that BT-7 is equivalent to about 120 times the safe dose for clinical adults (body weight of 70 kg) in the maximum tolerance test, and none of them showed acute toxicity.[40] In clinical observation studies, BT-7 has shown good efficacy in intestinal diseases caused by bacterial infections, and different research groups can repeat its effectiveness at different times and hospitals.[41–44]

Salmonellosis is a prevalent bacterial infection that specifically targets the gastrointestinal tract. *Salmonella* pathogens commonly settle in the gastrointestinal tract of humans and pass through in stools.[45] Humans are primarily affected through water or food that has been polluted. *S. Typhimurium* strains have demonstrated invasiveness by bypassing the intestinal wall and entering the bloodstream. This unique ability to cause disease is strongly associated with the virulence characteristics of *S. Typhimurium*.[46] *Salmonella* has pathogenic islands can mediate its invasion of intestinal epithelial cells. In order to clarify the effect of BT-7 on *Salmonella* virulence genes, RNA-Seq was used to compare gene expression on BT-7-treated or non-treated *Salmonella* cells. BT-7 downregulates 1547 genes in *Salmonella*, mainly arginine biosynthesis, *Salmonella* infection, and sulfur metabolism-related genes. Potential future antibiotic candidates are bacterial nutritional stress inhibitors. Amino acid biosynthesis pathways play a crucial role in bacterial growth under conditions of limited nutrients, both in laboratory

https://doi.org/10.2147/JIR.S491957

Table 2 The Key Antibacterial Components in Batri-7

NO.	Compound	Chemical Formula	Calculated m/z	Obtained m/z	Reported Inhibiting Bacteria
1	Nobiletin	$C_{21}H_{22}O_8$	402.1315	403.1373	*Helicobacter pylori*,[15] *Pseudomonas*[16]
2	Genistein	$C_{15}H_{10}O_5$	270.0528	271.0609	*Vibrio harveyi* and *Bacillus subtilis*[17]
3	Morin	$C_{15}H_{10}O_7$	302.0427	303.0504	*Vibrio cholerae*[18]
4	Oroxylin A	$C_{16}H_{12}O_5$	284.0685	285.0757	*Bacillus subtilis, Staphylococcus aureus, Klebsiella aerogenes* and *Pseudomonas aeruginosa*[19]
5	Apigenin	$C_{15}H_{10}O_5$	270.0528	271.0616	*Escherichia coli*[20]
6	Chrysin	$C_{15}H_{10}O_4$	254.0579	255.0657	*Escherichia coli, Salmonella typhimurium, Staphylococcus aureus*, and *Listeria monocytogenes*[21]
7	Quercetin	$C_{15}H_{10}O_7$	302.0427	303.0507	*Staphylococcus aureus* and *Escherichia coli*[22]
8	Rutin	$C_{27}H_{30}O_{16}$	610.1534	611.1621	*Klebsiella pneumoniae* and *Escherichia coli*[23]
9	Rhamnetin	$C_{16}H_{12}O_7$	316.0583	317.0662	*Escherichia coli*[24]
10	Kaempferol	$C_{15}H_{10}O_6$	286.0477	287.0557	*Staphylococcus aureus, Escherichia coli, Mycobacterium tuberculosis* and *Helicobacter pylori*[25]
11	Luteolin	$C_{15}H_{10}O_6$	286.0477	287.0556	*Staphylococcus aureus*[26]
12	Myricetin	$C_{15}H_{10}O_8$	318.0376	319.0453	*Staphylococcus aureus*[27]
13	Liquiritigenin	$C_{15}H_{12}O_4$	256.0736	257.0816	*Mycobacterium tuberculosis*[28]
14	Isoliquiritigenin	$C_{15}H_{12}O_4$	324.1362	325.1444	*Staphylococcus aureus, Staphylococcus epidermidis*, and *Staphylococcus hemolyticus*,[29] *Mycobacterium tuberculosis*,[28] *Mycobacterium bovis*[30]
15	Eriodictyol	$C_{15}H_{12}O_6$	288.0634	289.0715	*Micrococcus luteus, Staphylococcus aureus* and *Bacillus subtilis*[31]
16	Geranylgeraniol	$C_{20}H_{34}O$	290.261	291.2688	*Streptococcus mutans*[32]
17	Rhein	$C_{15}H_8O_6$	284.0321	285.0402	*Streptococcus mutans*[33]
18	Pterostilbene	$C_{16}H_{16}O_3$	256.1099	257.1165	*Staphylococcus aureus*[34]
19	Cholic acid	$C_{24}H_{40}O_5$	408.2876	431.2764	*Staphylococcus aureus* and *Escherichia coli*[35]
20	Deoxycholic acid	$C_{24}H_{40}O_4$	392.2927	393.2974	*Helicobacter pylori*[36]

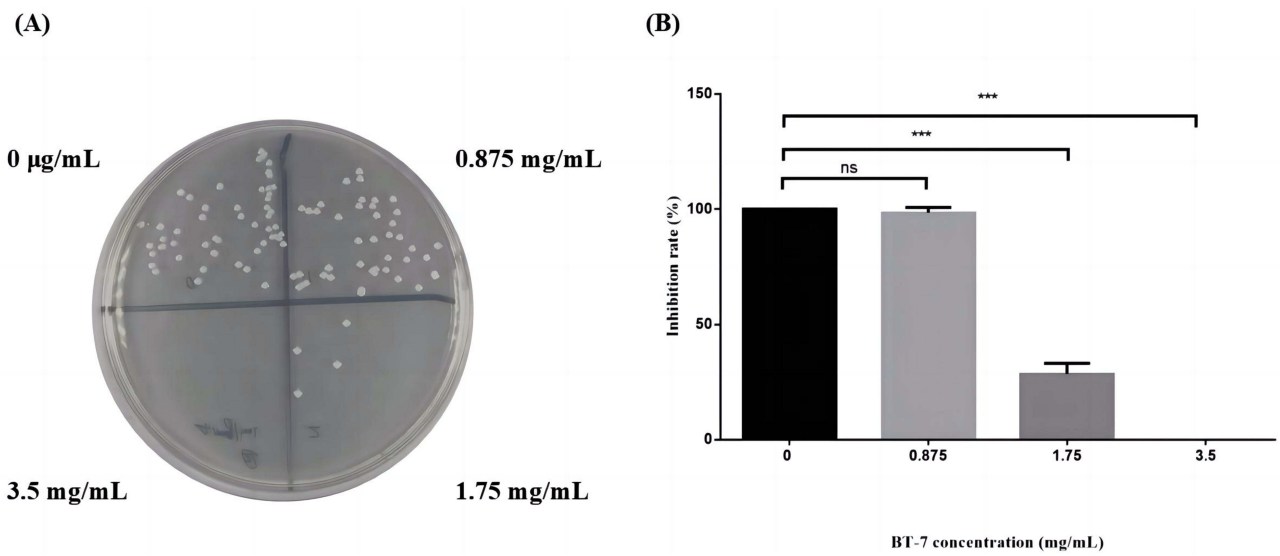

Figure 6 Antibacterial activity against *Salmonella* by BT-7. (**A**). Dose-dependent antibacterial study at the BT-7-SBE from 0 mg/mL up to 3.5 mg/mL. (**B**). Graph of mean inhibition rate from three times diffusion assays showing the effect of BT-7-SBE on the growth of *Salmonella* (triplicate experiments). The significance is given by $^{**}p < 0.001$; *ns*: non-significant ($p > 0.05$).

conditions and within the host.[47] BT-7 significantly downregulated arginine biosynthesis-related genes. The type III secretion system and effectors involved in epithelial cell invasion are encoded by the *Salmonella* enterica pathogenicity island 1 (SPI-1) gene cluster.[48] The SPI-1 genes (*sitA, sprB, hilC, sitB, hilA, sicP, hilD, sitC, invH, iagB, sptP, sitD, avrA, prgH, prgK, sipA*) is significantly downregulated by BT-7, which facilitates *Salmonella* infection in the host. Sulfur is an essential nutrient because of its impact on bacteria during colonization.[49] BT-7 significantly downregulated sulfur metabolism-related genes such as *cysD, cysP, cysK, cysT, cysN, cysJ*. Sulfur is a versatile element that may exist in various oxidation states. The redox activity of *Salmonella* is facilitated by this feature, which is present in the amino acid cysteine (Cys), methionine, and several important cofactors.[50] CysD and CysN-CysD are enzymes involved in ATP sulfurylation. CysN provides energy through its GTPase activity, allowing the formation of adenosine-5′-phosphosulfate. This compound can then enter the reductive branching of sulfate assimilation, subsequently leading to the production of cysteine.[51] BT-7 up-regulates 1522 genes in *Salmonella*, mainly ABC transporters, oxidative phosphorylation and o-Antigen nucleotide sugar biosynthesis pathway-related genes. Those genes contribute to *Salmonella* survival in antibacterial conditions. ABC transporters are commonly used by bacteria to develop resistance to antibiotics. These transporters actively remove the medicine from the cell.[52] The oxidative phosphorylation pathway of cellular respiration, which is involved in energy metabolism in bacteria, has become a novel target pathway for drug discovery.[53] Depending on the activation state, macrophages are divided into classically activated M1 macrophages and alternatively activated M2 macrophages. Gene expression correlates with macrophage type in *Salmonella*-induced macrophages. O-antigen nucleotide sugar biosynthesis pathway-related

Table 3 MIC of BT7 Against Three Types of Bacteria

Organism	MIC (mg/mL)
Salmonella typhimurium	3.5
Listeria monocytogenes	4
Staphylococcus aureus	2

https://doi.org/10.2147/JIR.S491957

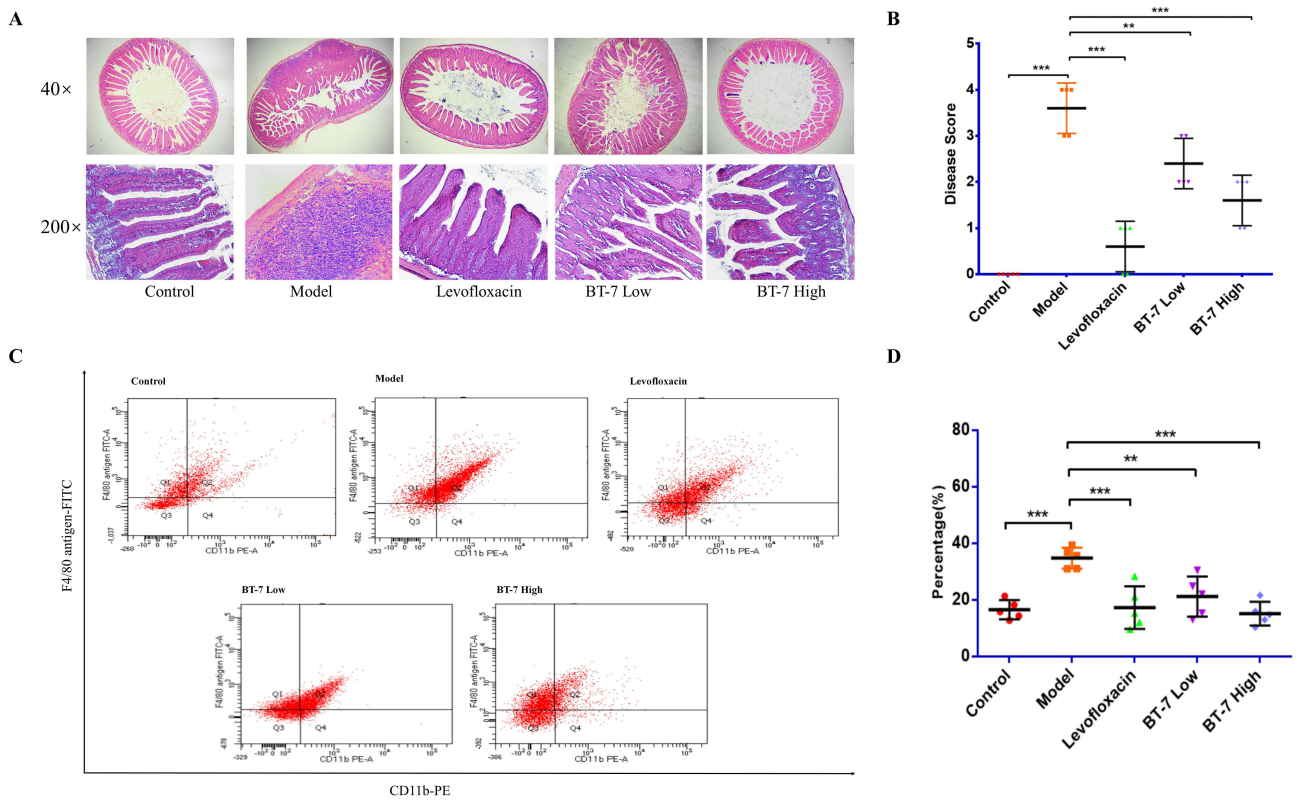

Figure 7 Histopathology analysis of small intestine from experimental mice after treated by BT-7 (H&E staining, 40 ×; 200 ×) and actions of BT-7 on the small intestine macrophages. Control, without infection normal small intestine tissue give equal volume saline; Model, small intestine tissue from mice infected with *Salmonella* treated with equal volume saline; Levofloxacin, positive control group, *Salmonella* infection mice treated with levofloxacin (20 mg/day); BT-7-Low, *Salmonella* infection mice treated with BT-7 (17.5 mg/day, 7 days); BT-7-High, *Salmonella* infection mice treated with BT-7 (35 mg/day, 7 days). (**A**) Histopathological changes were observed in the small intestine. (**B**) Histology scores of small intestinal of mouse. (**C**) and (**D**). Flow cytometry analysis has been performed to evaluate the expression of CD11b and F4/80 markers. Macrophages isolated from intestine tissue of mouse from Control, Model, Levofloxacin, BT-7-Low and BT-7-High groups were stained with antibodies against CD11b and F4/80 and isotype controls and analyzed by flow cytometry using the FACSDiva Software v8.0.1. The percentage of double-positive $CD11b^{+}$ /$F4/80^{+}$ events is in Q2. Results are expressed as mean ± SD (n = 5/group), $^{**}p$ <0.01, $^{***}p$ <0.001.

genes are highly expressed, allowing *Salmonella* to induce M1 macrophages.[54] *Salmonella* can survive and cause further infestation in both M1 and M2 macrophages,[55] and BT-7 reduces the number of total macrophages to help treat *Salmonella* infections.

In addition to TMM used in the treatment of infectious diseases in clinical practice, some of them have been found to be effective in the treatment of infection and inflammatory diseases in basic studies, such as the treatment of gastric ulcers with the drug Ruda-6.[56–58] The research on the treatment of bacterial infectious diseases is still in its infancy, and some of the TMM herb extracts have shown efficiency in the inhibition of *E. coli, S. aureus*, and *K. pneumoniae* growth.[59–61] In this study, we explore the mechanism of BT-7 against *Salmonella* infections, which is a new exploration in the field of TMM formulae against bacterial potential mechanisms. The TCM formulae San-Huang-Xie-Xin-Tang also has a therapeutic effect on *Salmonella* infection.[62] Therefore, the study and discovery of Traditional Medicines against bacterial infectious diseases can help to reduce the use of antibiotics and the production of drug-resistant bacteria.

Studying traditional formulations allows us to discover antimicrobial compounds and opportunities for multiple component combinations to cooperate inhibit bacterial growth. Our results show that BT-7 mainly regulates the inflammation-associated TNF signaling and Toll-like receptor signaling pathways. This may be related to the BT-7 containing key anti-inflammatory components. Studies have shown that morin,[63] quercetin,[64] myricetin,[65] luteolin,[66] rhein,[67] etc. can down-regulate the expression of inflammatory factor TNF-α. Nobiletin,[68] genistein,[69] morin,[70] apigenin,[71] myricetin,[72] etc. can inhibit toll-like receptor 4 pathway activation. The antimicrobial activity of BT-7 is

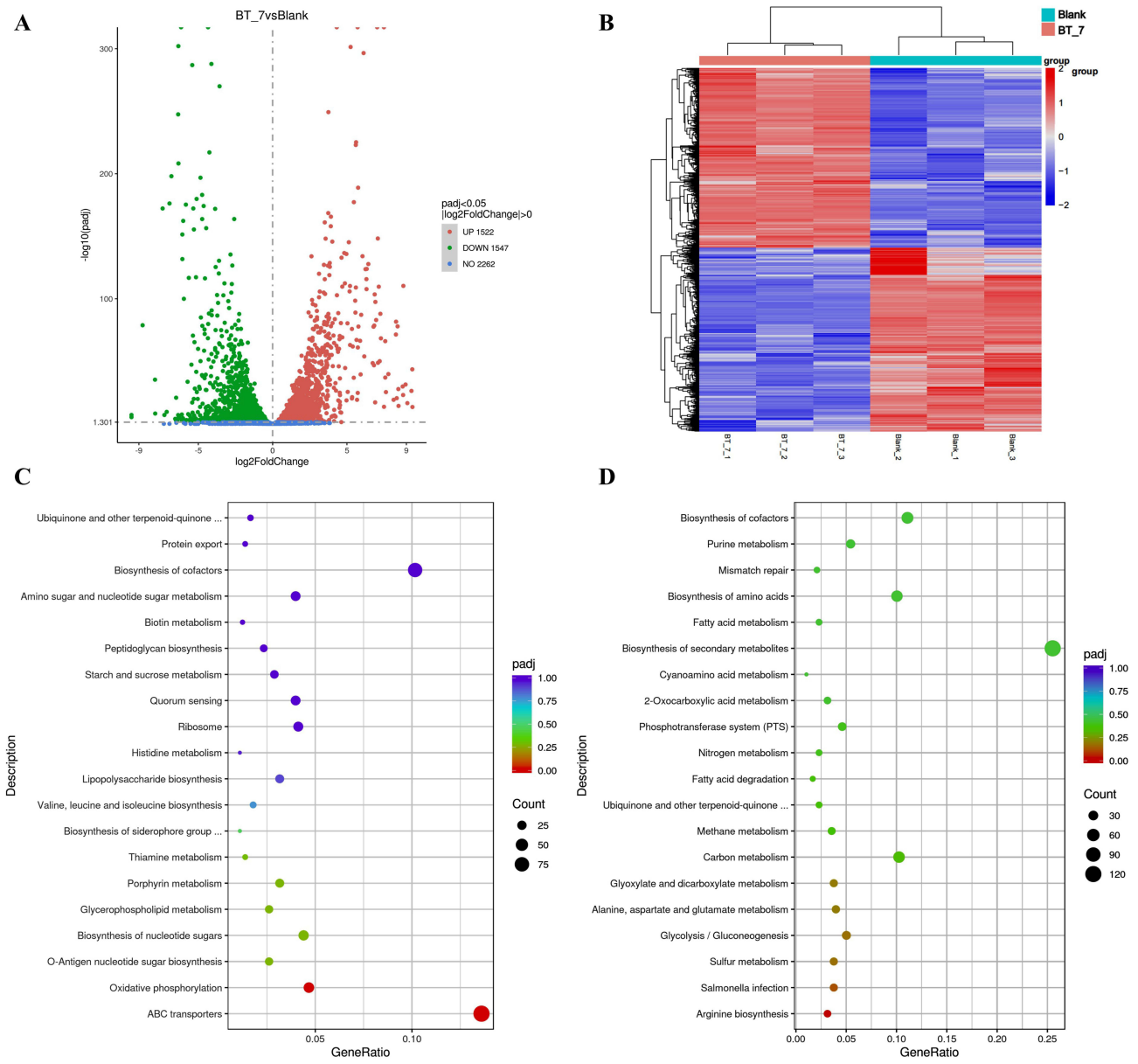

Figure 8 RNA-Seq analysis reveals genes and pathways targeted by BT-7. (**A**) Volcano plot of mRNAs expression in BT-7 treated (BT-7) and non-treated (Blank) group Salmonella cells (triplicate experiments). (**B**) Expression heatmap of differential expression genes between BT-7 treated (BT-7) and non-treated (Blank) group. (**C**) A barplot is used to display the enrichment of upregulated differentially expressed genes in KEGG. The X-axis indicates the count of genes, the Y-axis shows the different pathways, and the different colors reflect the corrected *P*-values. The graph displays the enrichment of upregulated DEGs in the KEGG database. The X-axis indicates the gene count, while the Y-axis represents the different pathways. The different colors on the graph indicate the corrected *P*-values, with a significance level of $p < 0.05$. (**D**) Barplot showing the enriched KEGG pathways of down-regulate DEGs.

related to its containment of flavonoids. These compounds have been shown to have antimicrobial effects, and some of them can inhibit drug-resistant strains.[24] Also, the combinations of those compounds will enhance each other's antibacterial effects.[73] Rutin enhanced antibacterial activities of flavonoids against *Salmonella enteritidis*.[74] Kaempferol combined with colistin against colistin-resistant gram-negative bacteria.[75] Therefore, we believe that the antibacterial and anti-inflammatory effects of BT-7 are the result of the combined action of these components.

https://doi.org/10.2147/JIR.S491957

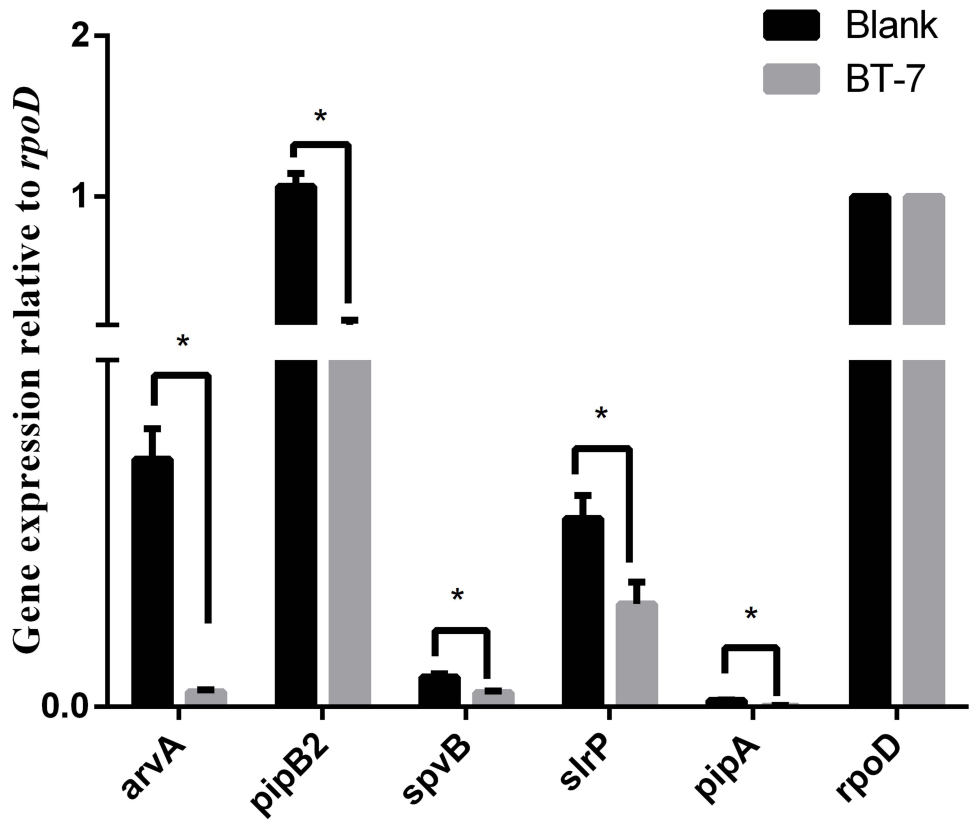

Figure 9 qRT-PCR confirmation of the BT-7 down-regulated genes. The mRNA level was determined in non-treated (Blank), BT-7 treated (BT-7) for 24 h. The mRNA amount of *rpoD* was set to 1 for calculation. Results shown are representative of three independent experiments and all values were mean ± standard deviation. *$p < 0.05$, vs none, *t*-test.

Conclusion

Collectively, our data suggest that BT-7 treats *Salmonella* induced enteritis through anti-inflammatory and anti-bacterial by TNF signaling pathway. BT-7 contains 20 anti-bacterial components to inhibit *Salmonella* growth through the target *Salmonella* infection genes.

Abbreviations

BT-7, Batri-7; LC-MS-MS: Liquid Chromatography with tandem mass spectrometry; HPLC, High-performance liquid chromatography; UPLC, Ultraperformance liquid chromatography; QTof-MS, Quadrupole time-of-flight mass spectrometry; MIC: Minimal inhibitory concentration; SPI, *Salmonella* pathogenicity island; WHO, World Health Organization.

Data Availability

RNA-seq raw data has been deposited in the NCBI BioProject database under accession number PRJNA1111718.

Funding

This research was kindly supported by Natural Science Foundation of Inner Mongolia Autonomous Region (2022ZD09, 2021ZD16), Inner Mongolia Medical and Health Science and Technology Plan (202202056), Science and Technology Program of the Joint Fund of Scientific Research for the Public Hospitals of Inner Mongolia Academy of Medical Sciences (2023GLLHD177) and Inner Mongolia Plan of Science and Technology (2020ZY0020).

Disclosure

The authors declare no conflicts of interest in this work.

References

1. Majowicz SE, Musto J, Scallan E, et al. The global burden of nontyphoidal salmonella gastroenteritis. *Clin Infect Dis*. 2010;50(6):882–889. doi:10.1086/650733
2. Zhao H, Zhao L, Wu F, Shen L. Clinical research on traditional Chinese medicine treatment for bacterial vaginosis. *Phytother Res*. 2021;35(9):4943–4956. doi:10.1002/ptr.7123
3. Li J, Feng S, Liu X, et al. Effects of traditional Chinese medicine and its active ingredients on drug-resistant bacteria. *Front Pharmacol*. 2022;13:837907. doi:10.3389/fphar.2022.837907
4. Xia H. Supplement and correction to the medicinal materials section of the Mongolian medicine division of the drug standards of the ministry of health of the People's Republic of China (Part 1). *Chin J Ethnic Med*. 2008;14(3):35–38.
5. Dezhi Y, Temuqile T. Research status and prospect of anti-bacterial properties of Mongolian traditional medicine batri7. *J Inner Mongolia Univ*. 2022;53(04):439–447. doi:10.13484/j.nmgdxxbzk.20220413
6. IMARDo H. Inner mongolia Mongolian patent medicine standards. Inner Mongolia Science Technology Press. 1984.
7. Hou PJ, Lin PY, Lin WL, Hsueh TP. Integrated traditional herbal medicine for recurrent urinary tract infection treatment and follow-up: a meta-analysis of randomized controlled trials. *J Ethnopharmacol*. 2024;321:117491. doi:10.1016/j.jep.2023.117491
8. Qin X, Wu Y, Zhao Y, et al. Revealing active constituents within traditional Chinese medicine used for treating bacterial pneumonia, with emphasis on the mechanism of baicalein against multi-drug resistant Klebsiella *pneumoniae*. *J Ethnopharmacol*. 2024;321:117488. doi:10.1016/j.jep.2023.117488
9. Wang R, Wu G, Du L, et al. Semi-bionic extraction of compound turmeric protects against dextran sulfate sodium-induced acute enteritis in rats. *J Ethnopharmacol*. 2016;190:288–300. doi:10.1016/j.jep.2016.05.054
10. Dou J, Sun X, Zhang Z, Yu D, Li C. Optimization of combination modes of medical materials in extract of Huanglian jiedu decoction by semi-bionic extraction. *Zhongguo Zhong Yao Za Zhi*. 2010;35(10):1256–1260. doi:10.4268/cjcmm20101009
11. Phuyal N, Jha PK, Raturi PP, Rajbhandary S. In vitro antibacterial activities of methanolic extracts of fruits, seeds, and bark of *Zanthoxylum armatum* DC. *J Trop Med*. 2020;2020:2803063. doi:10.1155/2020/2803063
12. Sekirov I, Tam NM, Jogova M, et al. Antibiotic-induced perturbations of the intestinal microbiota alter host susceptibility to enteric infection. *Infect Immun*. 2008;76(10):4726–4736. doi:10.1128/IAI.00319-08
13. Gaowa S, Bao N, Da M, et al. Traditional Mongolian medicine eerdun wurile improves stroke recovery through regulation of gene expression in rat brain. *J Ethnopharmacol*. 2018;222:249–260. doi:10.1016/j.jep.2018.05.011
14. Roulis M, Armaka M, Manoloukos M, Apostolaki M, Kollias G. Intestinal epithelial cells as producers but not targets of chronic TNF suffice to cause murine Crohn-like pathology. *Proc Natl Acad Sci USA*. 2011;108:5396–5401. doi:10.1073/pnas.1007811108
15. Ouyang Y, Li L, Ling P. Nobiletin inhibits *Helicobacterium pylori* infection-induced gastric carcinogenic signaling by blocking inflammation, apoptosis, and mitogen-activated protein kinase events in gastric epithelial-1 cells. *J Environ Pathol Toxicol Oncol*. 2020;39(1):77–88. doi:10.1615/JEnvironPatholToxicolOncol.2020031272
16. Yao X, Zhu X, Pan S, et al. Antimicrobial activity of nobiletin and tangeretin against Pseudomonas. *Food Chem*. 2012;132(4):1883–1890. doi:10.1016/j.foodchem.2011.12.021
17. Ulanowska K, Tkaczyk A, Konopa G, Wegrzyn G. Differential antibacterial activity of genistein arising from global inhibition of DNA, RNA and protein synthesis in some bacterial strains. *Arch Microbiol*. 2006;184(5):271–278. doi:10.1007/s00203-005-0063-7
18. Nag D, Dastidar DG, Chakrabarti G. Natural flavonoid morin showed anti-bacterial activity against Vibrio cholera after binding with cell division protein FtsA near ATP binding site. *Biochim Biophys Acta Gen Subj*. 2021;1865(8):129931. doi:10.1016/j.bbagen.2021.129931
19. Suresh Babu K, Hari Babu T, Srinivas PV, et al. Synthesis and in vitro study of novel 7-O-acyl derivatives of oroxylin A as antibacterial agents. *Bioorg Med Chem Lett*. 2005;15(17):3953–3956. doi:10.1016/j.bmcl.2005.05.045
20. Kim S, Woo ER, Lee DG. Apigenin promotes antibacterial activity via regulation of nitric oxide and superoxide anion production. *J Basic Microbiol*. 2020;60(10):862–872. doi:10.1002/jobm.202000432
21. Bi F, Yong H, Liu J, Zhang X, Shu Y, Liu J. Development and characterization of chitosan and D-α-tocopheryl polyethylene glycol 1000 succinate composite films containing different flavones. *Food Pack Shelf Life*. 2020;25:100531. doi:10.1016/j.fpsl.2020.100531
22. Jaisinghani R. Antibacterial properties of quercetin. *Microbiol Res*. 2017;8. doi:10.4081/mr.2017.6877
23. Wang Z, Ding Z, Li Z, Ding Y, Jiang F, Liu J. Antioxidant and antibacterial study of 10 flavonoids revealed rutin as a potential antibiofilm agent in Klebsiella pneumoniae strains isolated from hospitalized patients. *Microb Pathog*. 2021;159:105121. doi:10.1016/j.micpath.2021.105121
24. Lee H, Krishnan M, Kim M, Yoon YK, Kim Y. Rhamnetin, a natural flavonoid, ameliorates organ damage in a mouse model of carbapenem-resistant Acinetobacter *baumannii*-induced sepsis. *Int J mol Sci*. 2022;23(21). doi:10.3390/ijms232112895
25. Calderon-Montano JM, Burgos-Moron E, Perez-Guerrero C, Lopez-Lazaro M. A review on the dietary flavonoid kaempferol. *Mini Rev Med Chem*. 2011;11(4):298–344. doi:10.2174/138955711795305335
26. Wang Q, Xie M. Antibacterial activity and mechanism of luteolin on Staphylococcus aureus. *Wei Sheng Wu Xue Bao*. 2010;50(9):1180–1184.
27. Taheri Y, Suleria HAR, Martins N, et al. Myricetin bioactive effects: moving from preclinical evidence to potential clinical applications. *BMC Complement Med Ther*. 2020;20(1):241. doi:10.1186/s12906-020-03033-z
28. Chokchaisiri R, Suaisom C, Sriphota S, Chindaduang A, Chuprajob T, Suksamrarn A. Bioactive flavonoids of the flowers of *Butea monosperma*. *Chem Pharm Bull*. 2009;57(4):428–432. doi:10.1248/cpb.57.428
29. de Barros Machado T, Leal ICR, Kuster RM, et al. Brazilian phytopharmaceuticals – evaluation against hospital bacteria. *Phytother Res*. 2005;19(6):519–525. doi:10.1002/ptr.1696
30. Brown AK, Papaemmanouil A, Bhowruth V, Bhatt A, Dover LG, Besra GS. Flavonoid inhibitors as novel antimycobacterial agents targeting Rv0636, a putative dehydratase enzyme involved in mycobacterium tuberculosis fatty acid synthase II. *Microbiology*. 2007;153(Pt 10):3314–3322. doi:10.1099/mic.0.2007/009936-0
31. Chu LL, Pandey RP, Jung N, Jung HJ, Kim EH, Sohng JK. Hydroxylation of diverse flavonoids by CYP450 BM3 variants: biosynthesis of eriodictyol from naringenin in whole cells and its biological activities. *Microb Cell Fact*. 2016;15(1):135. doi:10.1186/s12934-016-0533-4
32. Wiart C, Kathirvalu G, Raju CS, et al. Antibacterial and antifungal terpenes from the medicinal angiosperms of Asia and the Pacific: haystacks and gold needles. *Molecules*. 2023;28(9):3873. doi:10.3390/molecules28093873

33. Folliero V, Dell'Annunziata F, Roscetto E, et al. Rhein: a novel antibacterial compound against streptococcus mutans infection. *Microbiol Res*. 2022;261:127062. doi:10.1016/j.micres.2022.127062
34. Tang KW, Yang SC, Tseng CH. Design, synthesis, and anti-bacterial evaluation of triazolyl-pterostilbene derivatives. *Int J mol Sci*. 2019;20 (18):4564. doi:10.3390/ijms20184564
35. Wu J, Yu TT, Kuppusamy R, et al. Cholic acid-based antimicrobial peptide mimics as antibacterial agents. *Int J mol Sci*. 2022;23(9). doi:10.3390/ijms23094623
36. Itoh M, Wada K, Tan S, Kitano Y, Kai J, Makino I. Antibacterial action of bile acids against helicobacter pylori and changes in its ultrastructural morphology: effect of unconjugated dihydroxy bile acid. *J Gastroenterol*. 1999;34(5):571–576. doi:10.1007/s005350050374
37. Popa GL, Papa MI. Salmonella spp. infection - a continuous threat worldwide. *Germs*. 2021;11(1):88–96. doi:10.18683/germs.2021.1244
38. Cui X, Lü Y, Yue C. Development and research progress of anti-drug resistant bacteria drugs. *Infect Drug Resist*. 2021;14:5575–5593. doi:10.2147/idr.S338987
39. Atanasov AG, Zotchev SB, Dirsch VM, et al. Natural products in drug discovery: advances and opportunities. *Nat Rev Drug Discov*. 2021;20 (3):200–216. doi:10.1038/s41573-020-00114-z
40. Li S, Bao L, Li S. Experimental Study on Anti-inflammatory Effects and Acute Toxicity of Mongolian Medicine Batri-7- Taking Effective Parts as Research Objects (article in Chinese). *World Sci Tech*. 2019;21(07):1393–1398.
41. Bao N. Study on the therapeutic effect of the Mongolian medicine Batri-7 in the treatment of bacillary dysentery (article in Chinese). *World's Newest Med Inform Digest*. 2018;18(94):170+178. doi:10.19613/j.cnki.1671-3141.2018.94.118
42. Erdenbrisi G. Three cases of acute abdominal diseases treated with the combination of western medicine and Mongolian medicine "Batri-7" (article in Chinese). *Northern Pharm*. 2017;14(04):192.
43. Batejin LJ, Wu C. Analysis of the efficacy of Mongolian medicine batri-7 in treating 84 cases of acute bacillary dysentery. *Chin J Ethnic Med*. 2012;18(10):17–18. doi:10.16041/j.cnki.cn15-1175.2012.10.012
44. Wulan T, Li Q, Discussion on the therapeutic efficacy of Mongolian medicine "Batri-7" in the treatment of pediatric diarrheal diseases (article in Chinese). *World's Newest Med Inform Digest*. 2016;16(30):129.
45. Canning M, Birhane MG, Dewey-Mattia D, et al. Salmonella outbreaks linked to beef, United States, 2012–2019. *Journal of Food Protection*. 2023;86(5):100071. doi:10.1016/j.jfp.2023.100071
46. Dos Santos AMP, Ferrari RG, Conte-Junior CA. Virulence factors in salmonella typhimurium: the sagacity of a bacterium. *Curr Microbiol*. 2019;76 (6):762–773. doi:10.1007/s00284-018-1510-4
47. Carfrae LA, Brown ED. Nutrient stress is a target for new antibiotics. *Trends Microbiol*. 2023;31(6):571–585. doi:10.1016/j.tim.2023.01.002
48. Sánchez-Romero MA, Casadesús J. Contribution of SPI-1 bistability to Salmonella enterica cooperative virulence: insights from single cell analysis. *Sci Rep*. 2018;8(1):14875. doi:10.1038/s41598-018-33137-z
49. Kies Paige J, Hammer Neal D. A resourceful race: bacterial scavenging of host sulfur metabolism during colonization. *Infect Immun*. 2022;90(5): e00579–21. doi:10.1128/iai.00579-21
50. Lensmire JM, Hammer ND. Nutrient sulfur acquisition strategies employed by bacterial pathogens. *Curr Opin Microbiol*. 2019;47:52–58. doi:10.1016/j.mib.2018.11.002
51. Poyraz Ö, Brunner K, Lohkamp B, et al. Crystal structures of the kinase domain of the sulfate-activating complex in mycobacterium tuberculosis. *PLoS One*. 2015;10(3):e0121494. doi:10.1371/journal.pone.0121494
52. Wilson Daniel N. The ABC of ribosome-related antibiotic resistance. *mBio*. 2016;7(3). doi:10.1128/mbio.00598-16
53. Bahuguna A, Rawat S, Rawat DS. QcrB in mycobacterium tuberculosis: the new drug target of antitubercular agents. *Med Res Rev*. 2021;41 (4):2565–2581. doi:10.1002/med.21779
54. Luo F, Sun X, Qu Z, Zhang X. Salmonella typhimurium-induced M1 macrophage polarization is dependent on the bacterial O antigen. *World J Microbiol Biotechnol*. 2016;32(2):22. doi:10.1007/s11274-015-1978-z
55. Wang X, Yang B, Ma S, et al. Lactate promotes Salmonella intracellular replication and systemic infection via driving macrophage M2 polarization. *Microbiol Spectr*. 2023;11(6):e02253–23. doi:10.1128/spectrum.02253-23
56. Qu S, Bao J, Ao W, Bai L, Borjigidai A. Mongolian medicine: history, development and existing problems. *Chin Herb Med*. 2022;14(3):345–355. doi:10.1016/j.chmed.2022.06.004
57. Nie MS, Li XH, Zhang S, et al. Screening for anti-influenza virus compounds from traditional Mongolian medicine by GFP-based reporter virus. *Front Cell Infect Microbiol*. 2024;14:1431979. doi:10.3389/fcimb.2024.1431979
58. Feng L, A. L, Bao T. An integrated network analysis, RNA-seq and in vivo validation approaches to explore the protective mechanism of Mongolian medicine formulae Ruda-6 against indomethacin-induced gastric ulcer in rats. *Front Pharmacol*. 2023;14:1181133. doi:10.3389/fphar.2023.1181133
59. Okba MM, Abdel Baki PM, Abu-Elghait M, et al. UPLC-ESI-MS/MS profiling of the underground parts of common Iris species in relation to their anti-virulence activities against *Staphylococcus aureus*. *J Ethnopharmacol*. 2022;282:114658. doi:10.1016/j.jep.2021.114658
60. Lee SB, Cha KH, Kim SN, et al. The antimicrobial activity of essential oil from dracocephalum foetidum against pathogenic microorganisms. *J Microbiol*. 2007;45(1):53–57.
61. Meng X, Li D, Zhou D, Wang D, Liu Q, Fan S. Chemical composition, antibacterial activity and related mechanism of the essential oil from the leaves of Juniperus *rigida* Sieb. et Zucc against Klebsiella *pneumoniae*. *J Ethnopharmacol*. 2016;194:698–705. doi:10.1016/j.jep.2016.10.050
62. Chang CH, Wang SC, Lee CY, et al. Influence of administration timing of san-huang-xie-xin-tang treatment on attenuating salmonella enterica serovar Typhimurium infection. *Environ Toxicol*. 2024;39(9):4298–4307. doi:10.1002/tox.24322
63. Kumar V, Kumar R, Gurusubramanian G, Rathore SS, Roy VK. Morin hydrate ameliorates Di-2-ethylhexyl phthalate (DEHP) induced hepatotoxicity in a mouse model via TNF-α and NF-κβ signaling. *3 Biotech*. 2024;14(7):181. doi:10.1007/s13205-024-04012-8
64. Li L, Jiang W, Yu B, et al. Quercetin improves cerebral ischemia/reperfusion injury by promoting microglia/macrophages M2 polarization via regulating PI3K/Akt/NF-κB signaling pathway. *Biomed Pharmacother*. 2023;168:115653. doi:10.1016/j.biopha.2023.115653
65. Wang X, Sun Y, Li P, et al. The protective effects of myricetin against acute liver failure via inhibiting inflammation and regulating oxidative stress via Nrf2 signaling. *Nat Prod Res*. 2023;37(5):798–802. doi:10.1080/14786419.2022.2089138
66. Ding X, Liu J, Chen X, Zhang XH. Exploring the mechanism of luteolin improving immune and inflammatory responses in systemic sclerosis based on systems biology and cell experiments. *Int Immunopharmacol*. 2024;138:112587. doi:10.1016/j.intimp.2024.112587

67. Zheng P, Tian X, Zhang W, et al. Rhein suppresses neuroinflammation via multiple signaling pathways in LPS-stimulated BV2 microglia cells. *Evid Based Complement Alternat Med*. 2020;2020:7210627. doi:10.1155/2020/7210627
68. Deveci Ozkan A, Kaleli S, Onen HI, et al. Anti-inflammatory effects of nobiletin on TLR4/TRIF/IRF3 and TLR9/IRF7 signaling pathways in prostate cancer cells. *Immunopharmacol Immunotoxicol*. 2020;42(2):93–100. doi:10.1080/08923973.2020.1725040
69. Ma W, Ding B, Yu H, Yuan L, Xi Y, Xiao R. Genistein alleviates β-amyloid-induced inflammatory damage through regulating Toll-like receptor 4/nuclear factor κB. *J Med Food*. 2015;18(3):273–279. doi:10.1089/jmf.2014.3150
70. Tian Y, Li Z, Shen B, Zhang Q, Feng H. Protective effects of morin on lipopolysaccharide/d-galactosamine-induced acute liver injury by inhibiting TLR4/NF-κB and activating Nrf2/HO-1 signaling pathways. *Int Immunopharmacol*. 2017;45:148–155. doi:10.1016/j.intimp.2017.02.010
71. Li H, Zhang H, Zhao H. Apigenin attenuates inflammatory response in allergic rhinitis mice by inhibiting the TLR4/MyD88/NF-κB signaling pathway. *Environ Toxicol*. 2023;38(2):253–265. doi:10.1002/tox.23699
72. Lv H, An B, Yu Q, Cao Y, Liu Y, Li S. The hepatoprotective effect of myricetin against lipopolysaccharide and D-galactosamine-induced fulminant hepatitis. *Int J Biol Macromol*. 2020;155:1092–1104. doi:10.1016/j.ijbiomac.2019.11.075
73. Amin MU, Khurram M, Khattak B, Khan J. Antibiotic additive and synergistic action of rutin, morin and quercetin against methicillin resistant staphylococcus aureus. *BMC Complement Altern Med*. 2015;15:59. doi:10.1186/s12906-015-0580-0
74. Arima H, Ashida H, Danno G. Rutin-enhanced antibacterial activities of flavonoids against bacillus cereus and salmonella enteritidis. *Biosci Biotechnol Biochem*. 2002;66(5):1009–1014. doi:10.1271/bbb.66.1009
75. Zhou H, Xu M, Guo W, et al. The antibacterial activity of kaempferol combined with colistin against colistin-resistant gram-negative bacteria. *Microbiol Spectr*. 2022;10(6):e0226522. doi:10.1128/spectrum.02265-22